Cranfield UNIVERSITY

College of Aeronautics Report No. CU/COA-2011/01
September 2011

Effects of nonlinear flight control system elements on aircraft manual control

M. M. Lone and A. K. Cooke

Dynamics, Simulation & Control Group
Department of Aircraft Engineering
School of Engineering
Cranfield University
Cranfield
Bedfordshire MK43 0AL
m.m.lone@cranfield.ac.uk

Abstract

This report presents the experimental method and results from a series of desktop simulation tests designed to investigate manual control characteristics of young and relatively inexperienced civil pilots (24 years average age and 66 hours flight experience). Subjects were asked to perform tasks during which they had to establish longitudinal control through pitch attitude shown on a primary flight display. A linear aircraft model coupled with nonlinear flight control system was used to produce realistic vehicle dynamics. Increased encroachment into nonlinear command gearing was found to make aggressive subjects resort to high levels of crossover regression. The combined effects of rate-limiting and nonlinear command gearing was observed only for demanding tasks during which over-control was a typical feature. The classical precision and bimodal models were used for an in-depth study of pilot dynamics observed during compensatory tasks. Model parameters were found through the definition of a constrained nonlinear optimisation problem. A single feedforward equalisation element was used for tracking tasks. It was found that subjects developed similar low frequency feedforward equalisations, whilst large inter-subject variations exist for high frequency equalisations. The resulting models also provided some insight into the Neal-Smith and Bandwidth handling qualities criteria. Actuator rate-limiting could not be directly correlated to any of the pilot model parameters.

Contents

List of Figures

List of Tables

1 Introduction

Single aisle aircraft make up most of the air traffic today and the increasing demand for air transport will most likely maintain this proportion. These aircraft tend to be crewed by a relatively young pilot population who have far less experience than those flying long haul wide-body types. The shear number of such aircraft has also meant that they encounter upset incidents more frequently[1]. At the same time, the majority of studies done in the fields of flight simulation and aircraft handling qualities have used highly trained and skilled pilots. In fact, the mediums of pilot feedback, such as the Cooper-Harper and pilot-induced oscillation (PIO) rating scales, require well trained test pilots. Therefore, there is a need to develop an understanding of control techniques employed by young and relatively inexperienced pilots.

This study aims to investigate the control characteristics demonstrated by these pilots when faced with the activation of nonlinear flight control system (FCS) components such as command gearing and actuator rate-limiting. Command gearing is the most common form of nonlinearity found on modern aircraft, often used to immediately shape pilot commands, whilst actuator saturation and rate-limiting are inherent in all actuation systems. The reader should refer to Fielding[2] for a detailed discussion on nonlinear flight control system components. Although methods using describing functions exist for the analysis and design of control systems with such nonlinear components, changes in pilot dynamics due to these components are still not very well understood.

This report describes work done in three areas: (1) the setup of manual control experiments, (2) summary of experimental results and, (3) the modelling approach to capture pilot control strategy.

2 Experimental setup

2.1 Procedure

This study was undertaken in two experimental stages. The preliminary stage involved tests conducted with a mixture of young pilots and engineering students to achieve the following aims:

1. Develop man-machine interface and simulation capability necessary to capture relevant dynamics.
2. Design and fine-tune tasks through direct testing of subjects.
3. Develop analytical tools necessary to post-process and study experimental data.
4. Study the effects of training.

Preliminary tests to investigate training effects were conducted for 14 subjects with an average age and experience of 25 years and 10 flying hours respectively. The subjects were presented with a sum-of-sines compensatory task (two minutes in duration) and root-mean-square (rms) error was taken as a performance indicator. It was found that the subjects stabilised their performance between 5 to 7 runs. However, the tasks were found to require considerable amount of concentration and therefore, fatigue became a major factor when deciding the number of training and experimental runs allowed per session for future tests.

The final experiment involved five trainee civil pilots with an average age and experience of 24 years and 66 hours respectively. They performed the following 11 tasks, each two minutes in duration:

1. Five compensatory tasks for training.
2. Three compensatory tasks with varying encroachments into command gearing nonlinearity.

3. Three tracking tasks with increasing rate limiting.

Fatigue effects were avoided by allowing a short break after each set of tasks.

Whether the young pilots were put under a high gain situation or not remains debatable. Although more so in simulation than during actual flight tests, it is very difficult to insure pilots maintain a consistent level of aggressiveness or introduce high gains into the pilot-vehicle system. Here, two subjects performed the tests alongside each other and both were informed of their and their counterpart's rms error at completion. It was hoped that this would result in competition and consequently induce the subjects to operate with higher gains. It should also be noted that the nature of the tasks were considerably different to that of manual control during normal flight. In this case, the pilots perceive and focus on only two variables at a given time. Therefore, the subject can apply control action based on only two feedback channels. Minimising the number of control variables in this manner limits attention allocation and allows the subject to develop a control structure with only error and error rate as inputs and stick deflection (δ_s) as the sole output.

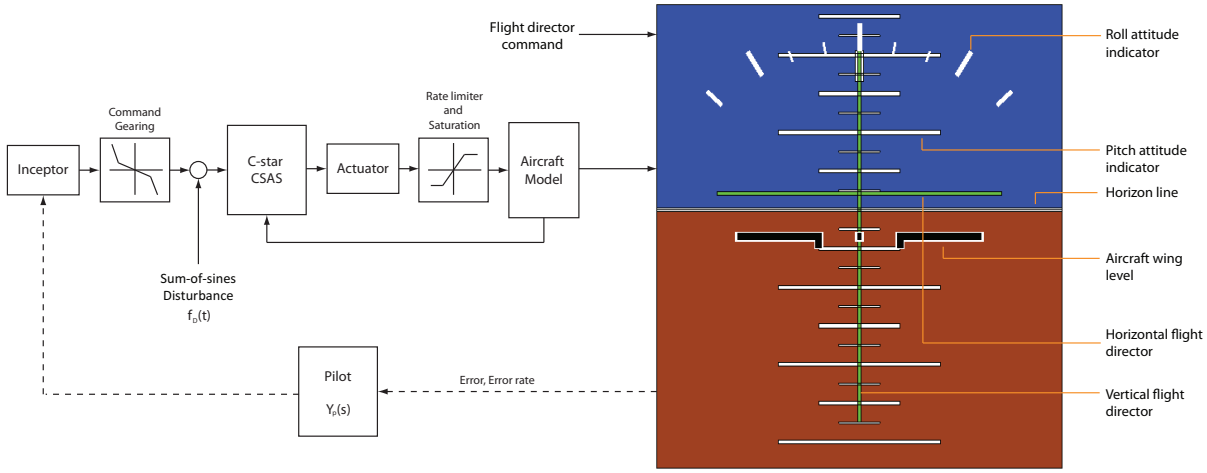

Figure 1: Experimental setup and display used for the experiments.

2.2 Aircraft model and hardware

The experimental setup used for both tracking and compensatory tasks is shown in Figure 1. A linear time invariant (LTI) model representative of a large four-engined transport aircraft during climb/approach (Mach 0.6, 28500 feet) was used[3]. A C-star control stability augmentation system (CSAS) was designed to present the subjects with dynamics representative of modern large transports. The FCS gains were selected such that aircraft response lay well within the Category 1 C-star boundary. Details of the aircraft model and dynamics can be found in Appendix A.

Aircraft pitch rate and attitude were presented to the pilot via a 110mm×115mm display shown in Figure 1. The attitude indicator scales were spaced such that 5° pitch attitude equalled a 10mm separation. All tests were conducted on laptops in a MATLAB/Simulink® environment with a nominal computational time delay of 13ms. The subjects performed tasks by manipulating Microsoft Sidewinder joysticks. The inactive nature of such an inceptor allows the relationship between pilot command and stick deflection to be kept relatively simple. Significant contribution to attenuation and phase lag was found only well above the manual control frequency range. At 5Hz, the joystick introduced negligible attenuation along with only 7° of phase lag.

Aircraft structural modes have been found to introduce phase lag and reduce the frequency of the short period pitch oscillatory mode[4].

2.3 Experimental tasks

All experiments involved the subjects performing either compensatory (disturbance rejection) tasks or tracking tasks in the aircraft longitudinal axis. When performing compensatory tasks, the flight director was switched off and the subjects tried to align the aircraft attitude indicator with the horizon line. Disturbance was injected, as shown in Figure 1, in the form of the following forcing function :

$$f_D(t) = \sum_{k=1}^{15} A_k \sin(\omega_k t + \phi_k) \tag{1}$$

Whilst being a relatively simple task, such a forcing function effectively excites the pilot's control action at selected frequencies over the desired frequency range. The phase (ϕ_k) for each sinusoid was randomised such that the subject could not perceive any internal coherence and thus adopt high level behaviour. A detailed discussion on the design of forcing functions can be found in work done by McRuer et al[5].

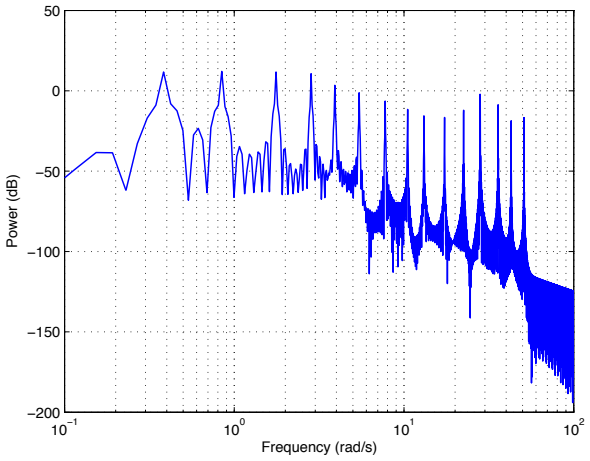

Figure 2: Power spectral density for the sum-of-sines forcing function.

Such a forcing function along with its corresponding pilot dynamics are well suited for the derivation of pilot's frequency response[6]. The raw time domain data was converted to frequency domain via the discrete fast Fourier transform. Pilot frequency response to a perceived variable was then derived as follows:

$$|Y_p(s)| = \frac{|\mathcal{F}\left[\delta_s(t)\right]|}{|\mathcal{F}\left[e_\theta(t)\right]|} \tag{2}$$

$$\angle Y_p(s) = \arg\mathcal{F}\left[\delta_s(t)\right] - \arg\mathcal{F}\left[e_\theta(t)\right] \tag{3}$$

The pilot-aircraft system was analysed in frequency domain via the superposition of the pilot and LTI model frequency responses. Crossover frequency is was obtained by noting the frequency at which the gain for the open-loop pilot-vehicle system was unity.

The tracking task required the pilot to follow the pitch attitude commands provided by the flight director. This demand comprised of a series of steps and ramps as shown in Figure 3.2 and is a modified version of the task used by Mitchell et al[7] in their investigation of rate-limiting effects.

k	A_k (deg.)	ω_k (rad/s)	k	A_k (deg.)	ω_k (rad/s)
1	0.13	0.38	9	0.03	13.12
2	0.13	0.84	10	0.03	17.33
3	0.13	1.76	11	0.04	22.46
4	0.12	2.84	12	0.06	28.12
5	0.08	3.91	13	0.05	35.88
6	0.06	5.45	14	0.03	42.78
7	0.04	7.75	15	0.03	50.96
8	0.03	10.51			

Table 1: Parameter values for sum-of-sines forcing function.

The forcing functions and the tracking tasks were kept relatively small in magnitude such that the LTI model remained valid. Limiting the study in this way meant that the inability to provide acceleration cues was made inconsequential.

3 Results

3.1 Command gearing

The effects of command gearing was investigated by presenting the subjects with a series of compensatory tasks. The following command gearing, similar to that used in modern civil aircraft, was used to convert the stick deflection to load factor demand:

$$\frac{N_{zc}}{\delta_s} = \begin{cases} -4, & -1.0 \leq \delta_{stick} \leq -0.5 \\ -1, & -0.5 < \delta_{stick} < 0.9 \\ -16, & 0.9 \leq \delta_{stick} \leq 1.0 \end{cases} \tag{4}$$

The subjects' control actions were forced to span over the nonlinear region by increasing the forcing function rms (σ_d). The effects are succinctly summarised in Figure 3. Increasing the number of incursions into the nonlinear region was found to make the task more difficult as evident by larger rms error. Most subjects maintained a crossover frequency of around 0.9rad/s, where as Subjects C and E resorted to different degrees of crossover regression. Adoption of greater crossover frequencies by Subject E indicates increased aggressiveness leading to degraded performance. Some insight can be gained by comparing Subject E's stick activity with that of Subject B in Figure 4(a). It shows the frequency with which the subjects encroach the nonlinear region. Subject E's aggressive control strategy leads to a cycle where every encroachment into the nonlinear region causes over-control which in turn, demands an equally aggressive recovery action. Therefore, the subject perceives high frequency oscillations in attitude and so maintains the greater crossover frequency. Thus, reinforcing the cycle.

3.2 Actuator rate-limiting

Actuator rate-limiting is known to introduce phase delay and amplitude attenuation into a closed-loop system[8]. A series of tracking tasks were used to investigate their affects on manual control. Tests were conducted with 25°/s, 35°/s and 45°/s actuator rate-limits. The command gearing described earlier was retained.

Upon hitting a rate-limit, subjects were found to compensate by increasing their gain (leading to larger stick deflections) to get the desired response. However, the introduced phase delay led to larger overshoots and longer recovery times. This can be seen around 43 seconds in Subject E's data, shown in Figure 3.2.

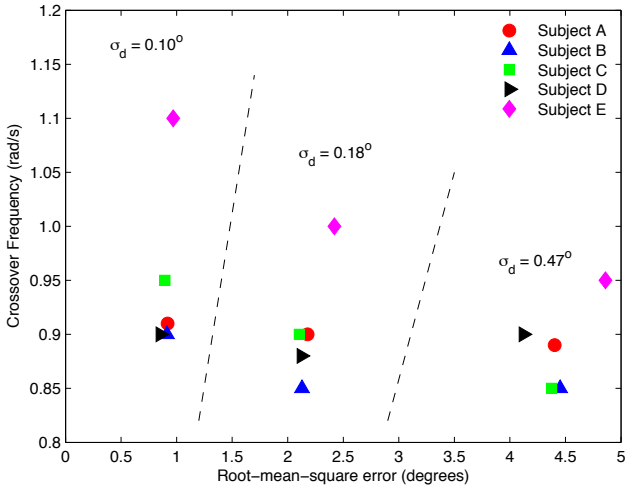

Figure 3: Effect of command gearing on subject performance.

The more demanding commands occurring at 42, 82 and 115 seconds led to the triggering of nonlinear command shaping causing actuator rate-limiting. This can be seen clearly in Figure 4(b).

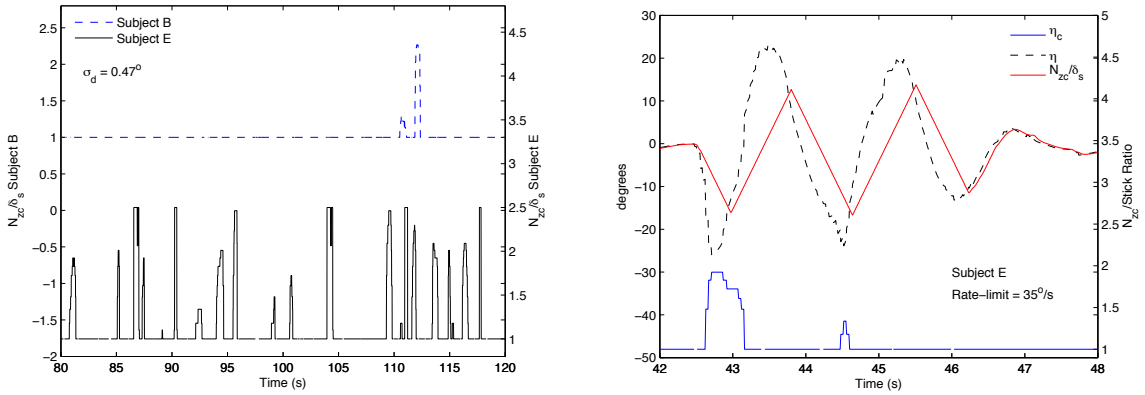

(a) Stick activity for Subjects B and E.

(b) Actuator performance and command gearing.

Figure 4: Comparison of stick activity and resulting rate-limiting.

By comparing the tracking performance at 42 seconds with that at 82 seconds, the subject can be seen to demonstrate learning and adaptability. Although this subject was found to be the most aggressive, the dynamics after the first minute is representative of the remaining subjects. They were found to apply gentle stick movements to track the flight director. Post-experiment feedback found that this characteristic was encouraged at the flight school.

4 Pilot model development

Pilot models can provide considerable insight into inter-subject variations in control characteristics. Differences in parameter values can highlight changes in subjective factors such as relative aggression and

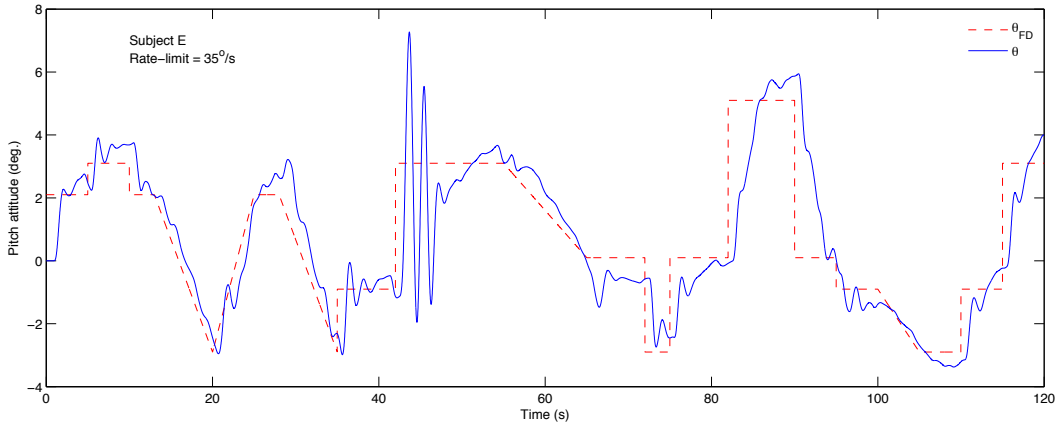

Figure 5: Tracking task and subject performance.

varying degrees in the understanding of vehicle dynamics. In this section, two types of classical pilot models are used for this purpose: the precision and bimodal models. For compensatory tasks these form the complete pilot model whilst for tracking tasks a feedforward path is added to the structure as shown in Figure 6. Reviews by Lone[9] and Grant[10] provide more detailed descriptions and comparisons of the pilot models used here.

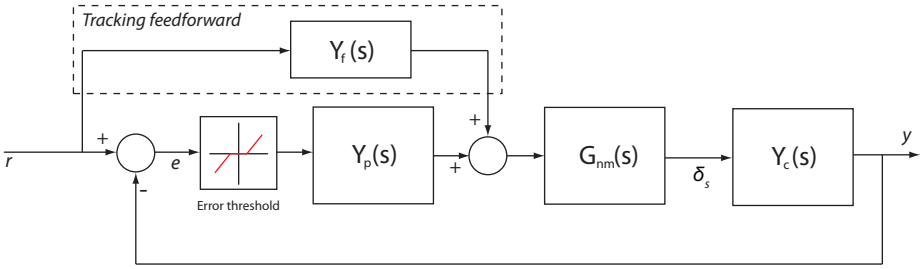

Figure 6: Pilot model structure for compensatory and tracking tasks.

4.1 Parameter identification method

The adopted approach uses nonlinear constrained optimisation to find model parameter values. The `fmincon` function in the MATLAB© optimisation toolbox was used here. Parameter bounds can be found in Appendix C Table 7. The following cost functions were initially used separately in the parameter identification process:

$$J_t(t) = \int_0^T |\delta_e - \delta_m|^2 dt \tag{5}$$

$$J_f(f) = \int_0^F |\Phi_e - \Phi_m|^2 df \tag{6}$$

where δ_e and δ_m are the experimental and model stick time histories and Φ_e and Φ_m are the corresponding power spectral densities.

Although $J_t(t)$ yielded parameter values that provided a good match between the model and experimental data for tracking tasks, the following cost function which was a composite of both frequency and time

domain errors was found to provide a better match for compensatory tasks:[1]

$$J_T(t,f) = \int_0^T |\delta_e - \delta_m|^2 dt + \Lambda \int_0^F |\Phi_e - \Phi_m|^2 df \quad (7)$$

$$= J_t(t) + \Lambda J_f(f) \quad (8)$$

Overall, eighteen experimental data sets were produced with subjects performing compensatory tasks. Ten of these were used for the parameter identification process and the remaining were used for validation. The parameter set corresponding to the best correlation was then used to fix the compensatory model. Similarly, out of the eighteen data sets where subjects were given tracking tasks, fifteen were used for identification and the remaining for validation. However, the search space for the tracking model parameters was limited by using the compensatory model found earlier.

4.2 Compensatory models

The classical precision model proposed by McRuer[11] represents the pilot as a single transfer function relating perceived attitude error to stick deflection:

$$Y_p(s) = K_p e^{-\tau s} \frac{(\tau_{\mathrm{L}} s + 1)(\tau_{\mathrm{LL}} s + 1)}{(\tau_{\mathrm{I}} s + 1)(\tau_{\mathrm{IL}} s + 1)} \quad (9)$$

This model assumes that the pilot adopts a structure that consists of two equalisations: (1) the typical equalisation observed during manual control to compensate for short period oscillation mode and (2) a low frequency equalisation for the phugoid mode.

	K_p	τ_{L}	τ_{LL}	τ_{I}	τ_{IL}	τ_n	ω_n	ζ_n	τ	$\lvert e_{th}\rvert$
Selected	0.12	0.65	0.56	1.72	0.01	0.08	10.00	0.25	0.24	0.45

Table 2: Selected precision model parameters.

The bimodal model is a simplified version of the model proposed by Hosman[10] and uses simple equalisations along both attitude error and error rate feedback paths:

$$Y_p(s) = \left[K_{p\theta} \frac{\tau_{\mathrm{L}\theta} s + 1}{\tau_{\mathrm{I}\theta} s + 1} + K_{pq} s \frac{\tau_{\mathrm{Lq}} s + 1}{\tau_{\mathrm{Iq}} s + 1} \right] e^{-\tau s} \quad (10)$$

	$K_{p\theta}$	$\tau_{\mathrm{L}\theta}$	$\tau_{\mathrm{I}\theta}$	K_{pq}	τ_{Lq}	τ_{Iq}	τ_n	ω_n	ζ_n	τ	$\lvert e_{th}\rvert$
Selected	0.02	-32.40	4.53	0.01	0.11	45.94	0.08	10.84	0.15	0.23	0.49

Table 3: Selected bimodal model parameters.

Any desired control action is finally implemented through the neuromuscular system, modelled here as:

$$G_{nm}(s) = \frac{\omega_n^2}{(\tau_n s + 1)(s^2 + 2\zeta_n \omega_n s + \omega_n^2)} \quad (11)$$

Although the experiments and tasks were designed such that the subject adopted a control strategy similar to that of a linear controller, the task nonetheless remains similar to that of manual control during turbulence. The careful design of forcing function ($f_D(t)$) can be credited for the excellent time and frequency domain matches shown in Figures 7 and 8 respectively. Similar matches were also obtained for all subjects hence, providing the basis for a quantitative study of pilot-vehicle stability and performance.

[1] For tracking and compensatory tasks the weighting was selected to be $\Lambda = 0$ and $\Lambda = 1000$ respectively.

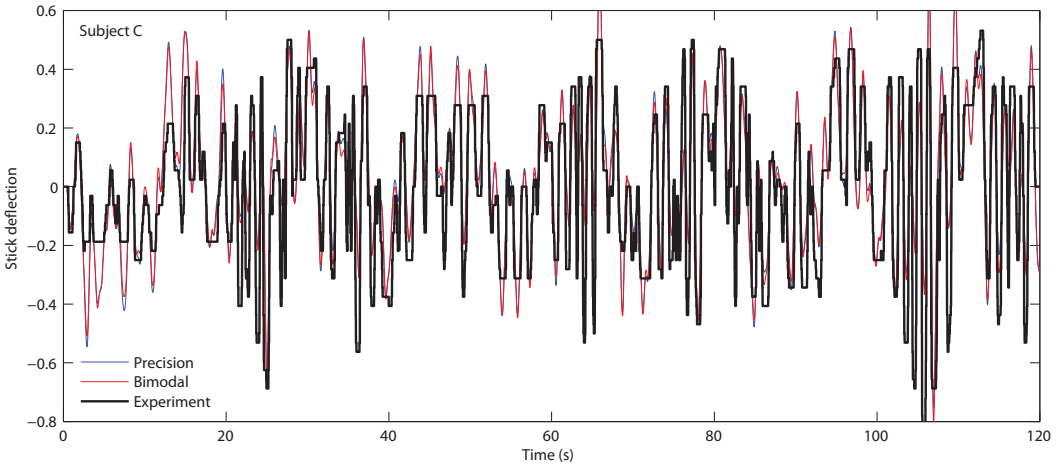

Figure 7: Example time-domain result from parameter identification process.

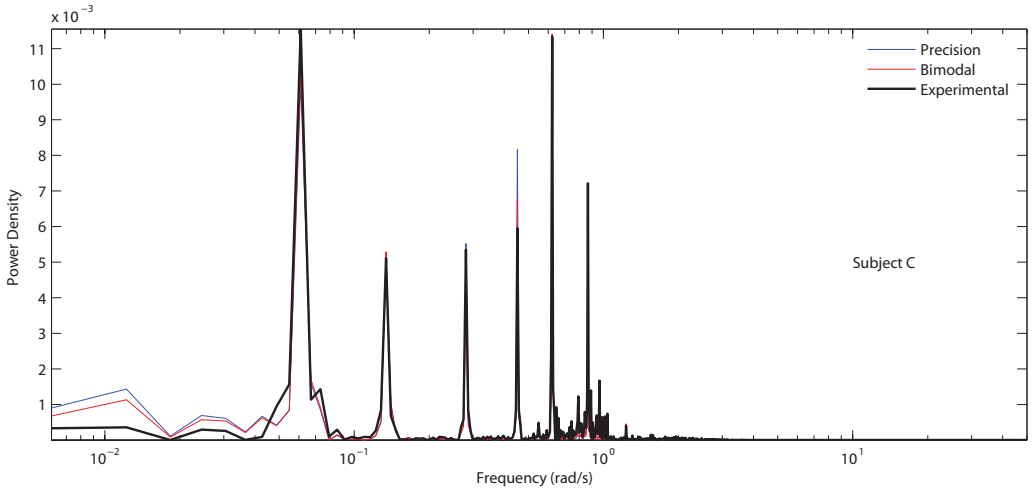

Figure 8: Example frequency-domain match for stick deflection.

	τ_n	ω_n	ζ_n
Selected	0.08	10.00	0.25

Table 4: Identified neuromuscular parameters

Insight into the effects of increased forcing function amplitude on adopted control strategies can be gained by comparing Subjects D and E in Figure 9; the ones with the minimum and maximum errors respectively. Subject E can be seen to increase lead generation for attitude tracking whilst dramatically reducing the lead for pitch rate tracking. Subject D, on the other hand, adopts the opposite strategy and achieves the better performance. Although, both subjects maintain roughly similar levels of attitude lag, Subject D increases his/her pitch rate lag far more than Subject E. Therefore, it can be said that focusing efforts into pitch attitude compensation along with limited crossover regression results in the best performance.

The frequency response for the selected pilot models, including the neuromuscular model, are shown in Figure 10 along with upper and lower bounds on gain and phase. Comparing these bounds shows that a greater variation exists for the precision model, indicating that the actual subjects follow the bimodal control strategy more closely. Therefore, it can also be said that subjects base their control action on

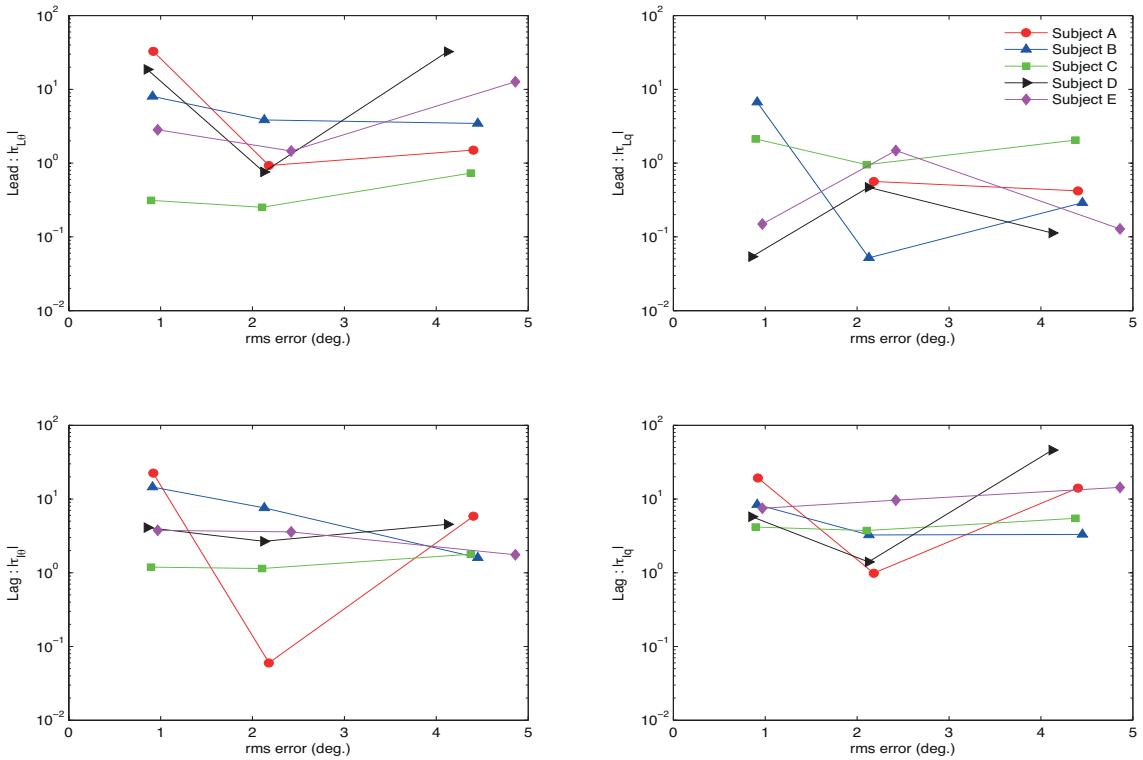

Figure 9: Variation of bimodal model lead and lag parameters with rms error.

both perceived pitch attitude and pitch rate.

4.2.1 Perspectives on handling qualities

To date, only the Neal-Smith and the approach introduced by Zeyada et al[12] (which uses the *handling qualities sensitivity function* (HQSF)) are the criteria that explicitly use a pilot model. On the other hand, the Bandwidth criterion includes pilot dynamics implicitly through the assumption used to define phase bandwidth. It is defined as the frequency for which the open loop pilot-vehicle phase is -135°, i.e. it assumes the pilot introduces an additional 45° of phase lag. Inspection of the pilot-vehicle system frequency response, shown in Figure 11, allows some discussion on the effects of subject dynamics on open-loop pilot-vehicle dynamics and also the basis of the existing frequency domain Neal-Smith and Bandwidth criteria. Effects due to pilot introduced dynamics are quite dramatic: (a) the crossover frequency is shifted back from 8.4rad/s to around 0.2rad/s and, (b) almost 40% of the phase improvement due to the CSAS is lost.[2]

The Neal-Smith pilot model is based on McRuer's classical pilot modelling approach from the early 1960's, whilst the HQSF method relies on the structural model developed by Hess in the 1990's. The following observations can be made when considering the closed-loop pilot-vehicle frequency response in the context of the Neal-Smith requirements:

1. The system bandwidth for both pilot models are between 2.74rad/s and 3.23rad/s. So it can be said that the requirement to fix the closed-loop bandwidth at 3.5rad/s is for a more aggressive pilot, leading to a more conservative criterion.

[2]Effects due to the EFCS can be seen in Appendix A Figure 15. The maximum phase improvement of 60° occurs at approximately 3.0rad/s.

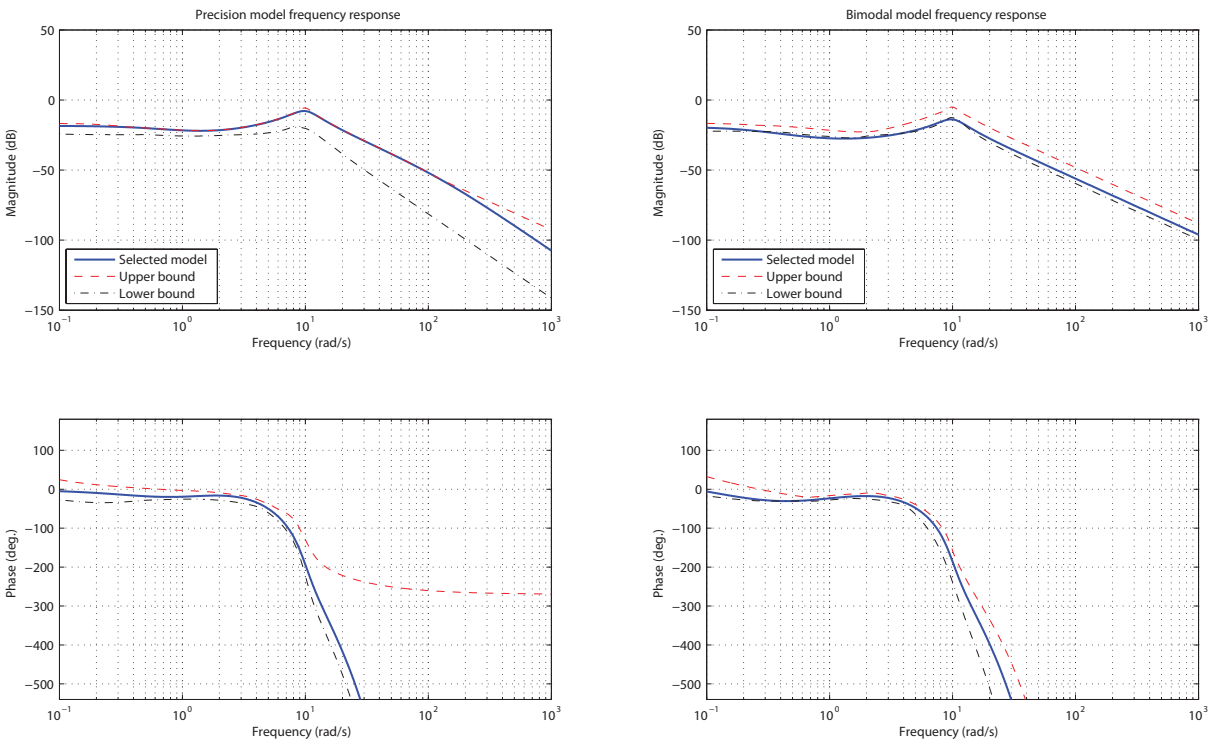

Figure 10: Frequency responses for compensatory pilot models.

2. The maximum low frequency droop with the precision and bimodal pilot models were found to be -8.52dB and -12.99dB respectively. Therefore, the requirement to fix the maximum low frequency droop at -3dB is non-conservative; the pilots involved in the experiments took much longer to settle aircraft nose onto the desired attitude.

3. The requirement to minimise the resonant peak was also found to be non-conservative, especially from the perspective of PIO. PIO susceptibility of such a configuration is highlighted by the insufficient gain attenuation and the resulting small gain margin.[3]

Application of the Bandwidth criterion to the open-loop dynamics was found to only confirm the popularity of this criterion[13]. Gain and phase bandwidths were found to be 4.94rad/s and 4.59rad/s. The open-loop pilot-vehicle system bandwidth (the frequency at -180° phase) was found to equal the phase bandwidth because 44.30° of phase delay was introduced by the pilot; validating the criterion's assumption that the pilot adds 45° phase lag.

4.3 Tracking models

The tracking model assumes the subject implements a feedforward loop with lead-lag compensation along with the same compensatory dynamics discussed in Section 4.2. Given the tracking pilot model structure of Figure 6, the linear relationship between the reference signal and stick deflection can be written as follows:

$$\frac{\delta_s(s)}{r(s)} = \frac{1 + Y_f(s)}{1 + Y_p(s)Y_c(s)} G_{nm}(s) \tag{12}$$

[3]The large inter-subject variations evident in the magnitude plots of Figure 10 and the small sample size of pilots predict that this configuration is even more PIO prone. Figure 11 also highlights the potential for aeroelastic aircraft-pilot-coupling due to low wing stiffness that may further reduce the frequency of the first wing bending mode.

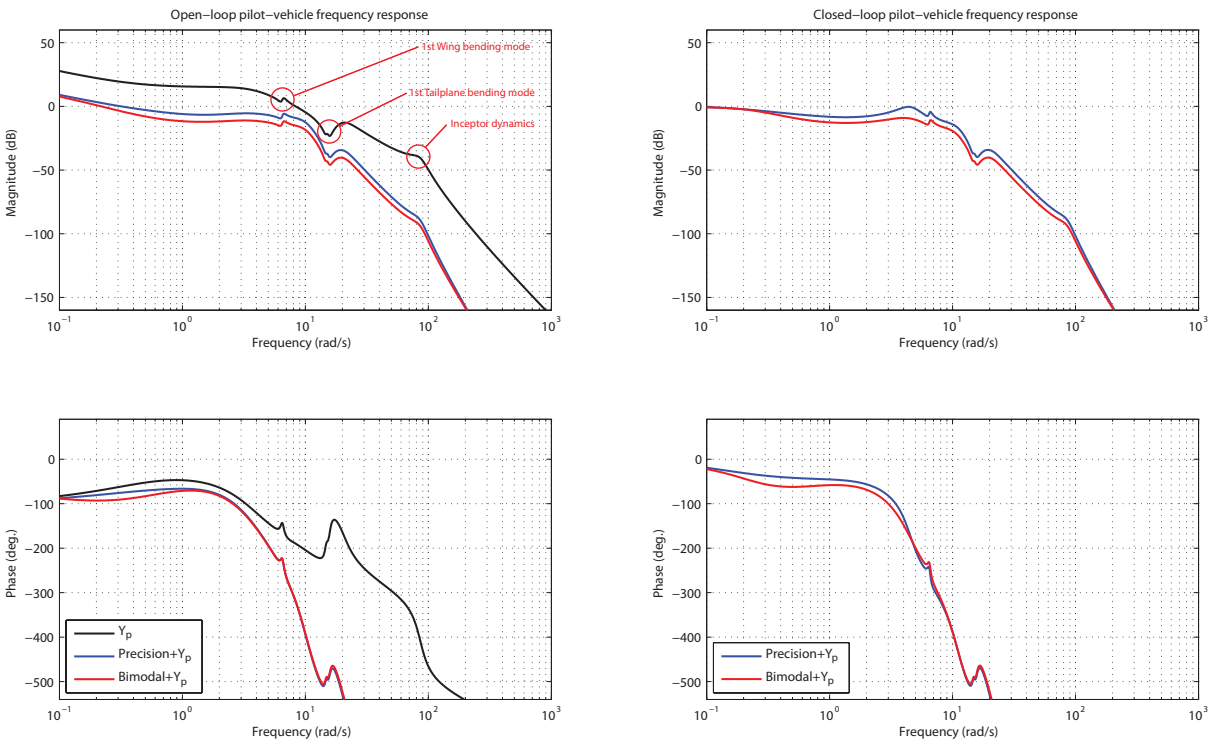

Figure 11: Pilot-vehicle system frequency responses.

where the feedforward equalisation is modelled as the following transfer function:

$$Y_f(s) = K_f \frac{\tau_{\mathrm{Lf}} s + 1}{\tau_{\mathrm{If}} s + 1} \frac{\tau_{\mathrm{LLf}} s + 1}{\tau_{\mathrm{ILf}} s + 1} e^{-\tau s} \tag{13}$$

It should be noted that this uses the same time delay as the compensatory loop. Such a formulation leads to a five parameter identification process. Example time histories with model parameters derived from the identification process are shown in Figure 12 and the corresponding parameter values are presented in Table 5; demonstrating that this approach can provide very satisfactory matches with experimental data. This feedforward equalisation augments both compensatory models. The high gain compensatory dynamics associated with the precision model are also evident in the form of the larger overshoots and more oscillatory stick movements. The complete results from the parameter identification process can be found in Appendix C Tables 8 and 9.

Compensatory model	K_f	τ_{Lf}	τ_{If}	τ_{LLf}	τ_{ILf}
Precision	-0.02	-21.10	1.06	-	-
Bimodal	-0.01	-30.40	-0.74	3.50	0.88

Table 5: Selected feedforward parameter values with precision and bimodal compensatory models.

The correlation between the stick deflections recorded during the experiments and the output from the model (produced using the experimental reference and error signals as inputs) can be used as a measure of how well the model reproduces pilot dynamics. Corresponding average values of 0.88 for the precision and 0.87 for the bimodal model imply that both capture the subjects' behaviour very effectively. However, the parameter identification process found that the feedforward model required to augment the precision model reduced to a first order equalisation for all subjects (see Appendix C Table 8). This implies that a simple lead-lag combination may be implemented in the feedforward path when using a single-input-single-output pilot model.

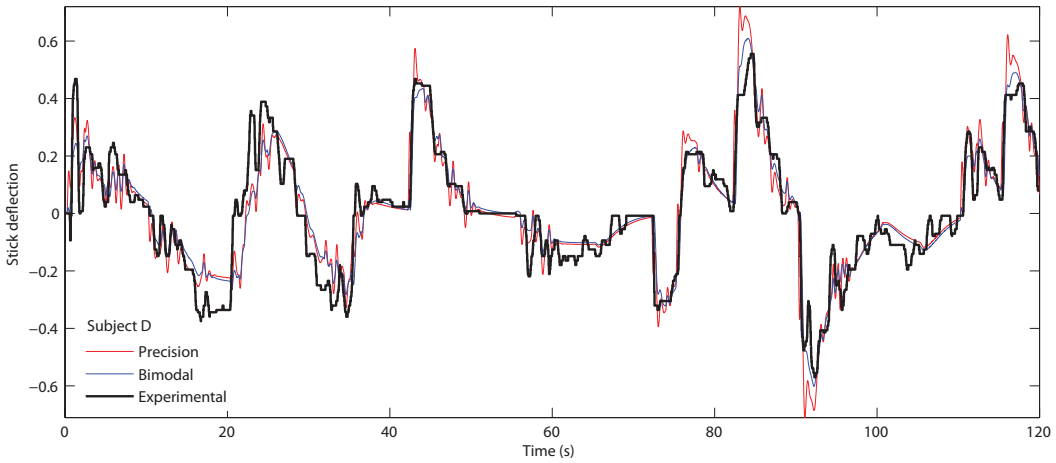

Figure 12: Tracking model comparison with Subject D stick deflection.

Studying the feedforward parameters gives insight into cases of over-control previously discussed in Section 3.2. Figure 13 shows inter-subject variation in lead and lag parameters and highlights the parameters for which over-control occurred. The values accociated with the bimodal model provides greater insight into the relationship between the adopted control strategies and over-control cases, especially in comparison with results from the precision model.[4] The following points can be deduced from Figures 13(c) and 13(d):

1. All cases of over-control may be attributed to insufficient equalisation at high frequencies.
2. No relationship between actuator rate-limiting and over-control can be found.
3. Inter-subject differences in low frequency equalisation is relatively small in comparison with the large variation in high frequency lead-lag generation.
4. There exists a relationship (possibly linear) between the adopted high frequency lead and lag parameters which, requires further investigation.

5 Conclusions

The experimental method and results from a series of desktop simulation tests designed to investigate the manual control characteristics of young and relatively inexperienced pilots has been presented. Five subjects with an average age and experience of 24 years and 66 hours respectively were asked to perform a series of simple control tasks. Compensatory and tracking tasks were used to study the effects of nonlinear command gearing and actuator rate-limiting. A linear aircraft model coupled with nonlinear flight control system was used to produce realistic vehicle dynamics. Increased encroachment into the nonlinear gearing was found to make aggressive subjects resort to a high degree of crossover regression. The combined effects of rate-limiting and nonlinear command gearing was observed only for demanding tasks during which over-control was a typical feature. The experimental data was then used for pilot model parameter identification. This was done by defining the identification process as a constrained nonlinear optimisation problem.

[4]With the exception of Subject A all subjects caused actuator rate-limiting, demonstrating the effectiveness of the tracking task for exposing the effects of actuator rate-limiting.

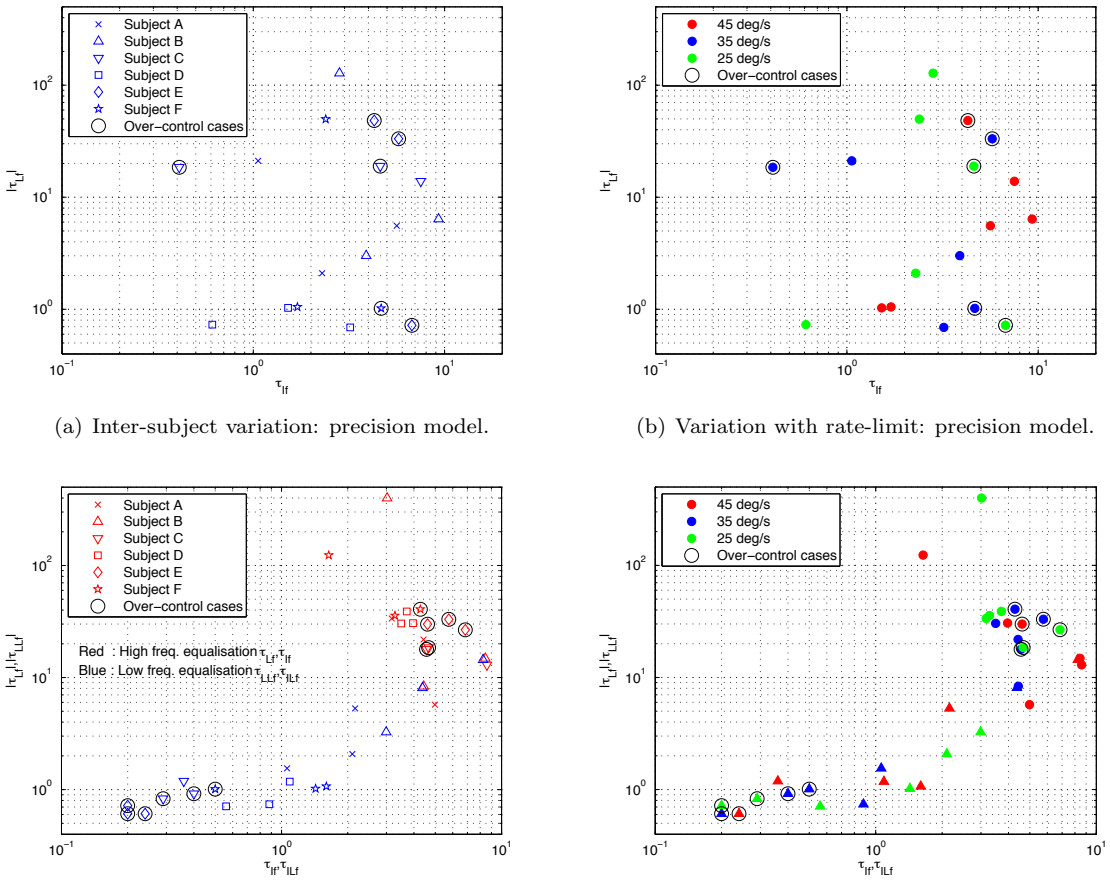

(a) Inter-subject variation: precision model.

(b) Variation with rate-limit: precision model.

(c) Inter-subject variation: bimodal model.

(d) Variation with rate-limit: bimodal model.

Figure 13: Variation of subject generated lead and lags along with cases of over-control.

Such a study of pilot control dynamics, that focuses on young and relatively inexperienced pilots, highlights the necessity to review handling qualities criteria and their implementation; especially now as airlines order large numbers of single-aisle aircraft and the demand for pilots is rocketing. Here, the Neal-Smith and Bandwidth critirea were reviewed. Apart from validating the pilot introduced phase lag assumption in the Bandwidth critrion, it was found that Neal-Smith requirements of -3dB droop and minimum resonant peak for selecting pilot model parameters were not conservative.

These experiments have not only allowed a qualitative study of pilot dynamics, but also paved the way to quantify inter-subject variations in pilot equalisation. Future work consists of expanding the experimental database by testing more subjects. It is also hoped that a comparison with older and more experienced pilot can be made. Another area that requires particular attention is the development of nonlinear manual control theory.

6 References

[1] A.A. Lambregts, G. Nesemeier, J.E. Wilborn, and R.L. Newman. Airplane upsets: old problem, new issues. In *AIAA Modelling and simulation technologuies conference and exhibit*, 2008.

[2] C. Fielding and P.K. Flux. Non-linearities in flight control systems. *The Aeronautical Journal*, 107:673–696, 2003.

[3] S. Andrews and A. Cooke. An aeroelastic flexible wing model for aircraft simulation. In *48th AIAA Aerospace Sciences Meeting Including the New Horizons Forum and Aerospace Exposition, Orlando, Florida, Jan. 4-7, 2010*, 2010.

[4] M.M. Lone and A.K. Cooke. Development of a pilot model suitable for the simulation of large aircraft. In *27th International Congress of the Aeronautical Sciences*, 2010.

[5] D.T. McRuer, D. Graham, and E.S. Krendel. Human pilot dynamics in compensatory systems: Theory, models, and experiments with controlled element and forcing function variations. Technical Report AFFDL-TR-65-15, Air Force Flight Dynamics Laboratory, 1965.

[6] M. Tischler and R. Remple. *Aircraft and Rotorcraft System Identification*. American Istitute of Aeronautics and Astronautics Inc., 2006.

[7] D.G. Mitchell, B.A. Kish, and J.S. Seo. A flight investigation of PIO due to rate limiting. In *IEEE Aerospace Conference*, 1998.

[8] D.G. Mitchell and E.J. Field. Nonlinearities and PIO with advanced aircraft control systems. In *Active Control Technology for Enhanced Performance Operational Capabilities of Military Aircraft, Land Vehicles and Sea Vehicles*, 2000.

[9] M.M. Lone and A.K. Cooke. Review of pilot modelling techniques. In *48th AIAA Aerospace Sciences Meeting Including the New Horizons Forum and Aerospace Exposition*, number AIAA-2010-297, Orlando, Florida,, January 2010.

[10] P. Grant and J. Schroeder. Modeling pilot control behaviorfor flight simulator design and assessment. In *AIAA Modeling and Simulation Technologies Conference, Toronto, Ontario, Aug. 2-5, 2010*, 2010.

[11] D.T. McRuer. Development of pilot-in-the-loop analysis. *Journal of Aircraft*, 10:515–524, 1973.

[12] Y. Zeyada and R.A. Hess. Modeling the human pilot in single-axis linear and nonlinear tracking tasks. In *Pilot-Induced Oscillation Research : Status at the End of the Century*, 2001.

[13] National Research Council. *Aviation Safety and Pilot Control - Understanding and Preventing Unfavorable Pilot-Vehicle Interactions*. National Academy Press, 1997.

A Aircraft model

A linearised state-space model for the aircraft was used in the experiments :

$$\begin{aligned} \dot{x} &= \mathbf{A}x + \mathbf{B}u \\ y &= \mathbf{C}x + \mathbf{D}u \end{aligned} \tag{14}$$

where,

$$x = \begin{bmatrix} \phi & \theta & \psi & u_b & v_b & w_b & p & q & r & \sigma_1 & \dots & \sigma_{24} \end{bmatrix}' \tag{15}$$

$$u = \eta \tag{16}$$

$$y = \begin{bmatrix} \theta & q & N_z \end{bmatrix}' \tag{17}$$

C-star flight control system and augmented aircraft step response:

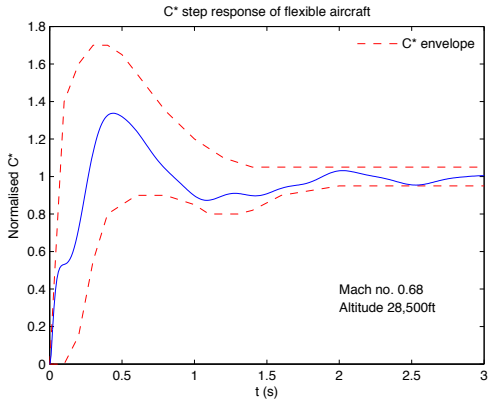

Figure 14: Step response of augmented aircraft.

Aircraft pitch attitude frequency response :

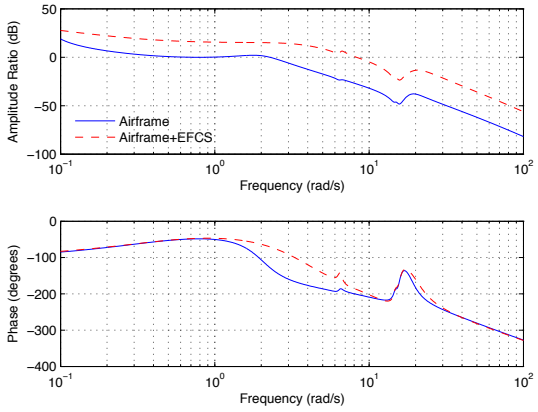

Figure 15: Aircraft pitch attitude frequency response with and without EFCS.

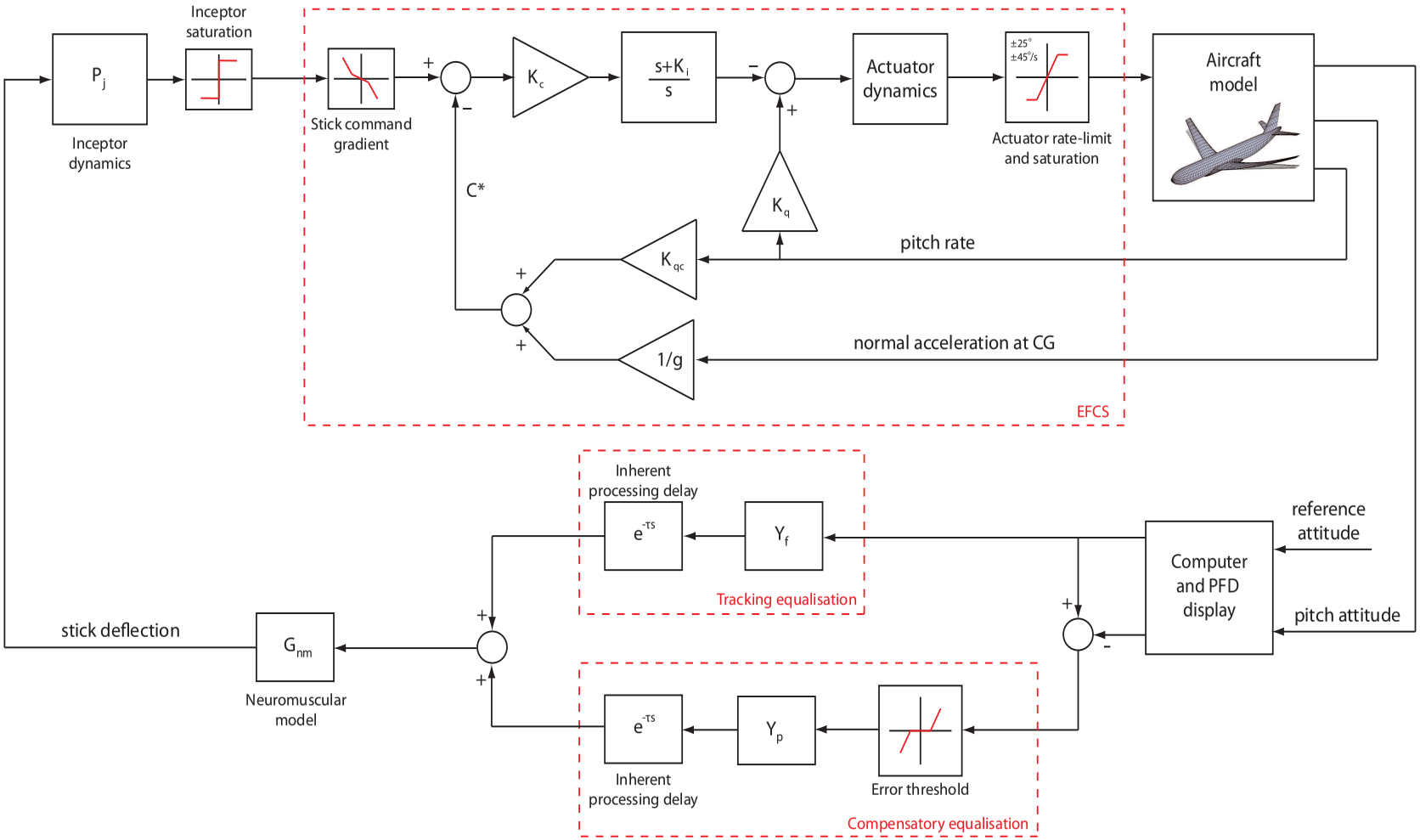

Figure 16: Modelling block diagram for the pilot-vehicle system in this study.

B Details of test subjects

Subject	Gender	Age (yrs)	Flight experience (hrs)	Aircraft type
A	M	25	25	PA28, DA40
B	M	21	10	PA28
C	M	25	250	PA28, PA44, DA40, DA44
D	M	25	30	DA40
E	M	18	15	DA40
Average	-	23.8	66	-

Table 6: Subject details.

Figure 17: Subjects performing experimental tasks.

C Pilot model parameter identification

Parameter	Min.	Max.
K_p,$K_{p\theta}$,K_{pq},K_f	$-\infty$	∞
τ_{L},τ_{LL},$\tau_{\mathrm{L}\theta}$,τ_{Lq},τ_{Lf},τ_{LLf}	$-\infty$	∞
τ_{I},τ_{IL},$\tau_{\mathrm{I}\theta}$,τ_{Iq},τ_{If},τ_{ILf}	0	∞
e_{th}	-2.50	2.50
τ	0	0.50
τ_n	0.08	0.10
ω_n	10	20
ζ_n	0.15	0.30

Table 7: Pilot model parameter constraints used for the identification process.

Subject	Run	K_f	τ_{Lf}	τ_{LLf}	τ_{If}	τ_{ILf}	Correlation
A	1	-0.039	-5.56	-5.40	5.62	-5.40	0.82
	2	-0.018	-21.10	-1.56	1.06	-1.56	0.92
	3	-0.010	-2.10	-33.56	2.29	-33.56	0.90
B	1	0.002	-6.38	372.87	9.30	372.87	0.71
	2	-0.008	-3.01	-52.31	3.89	-52.31	0.88
	3	0.002	127.89	-3.16	2.82	-3.16	0.87
C	1	-0.034	-13.88	-1.16	7.51	-1.16	0.89
	2	-0.020	-18.48	-0.92	0.41	-0.92	0.90
	3	-0.020	-18.93	-0.82	4.61	-0.82	0.89
D	1	0.002	-1.03	166.71	1.52	166.71	0.90
	2	-0.011	-0.69	-35.08	3.21	-35.08	0.91
	3	-0.010	-0.73	-39.31	0.61	-39.31	0.91
E	1	-0.009	-48.39	-0.58	4.29	-0.58	0.88
	2	-0.015	-33.23	-0.61	5.75	-0.61	0.86
	3	-0.019	-0.72	-27.30	6.75	-27.30	0.89

Table 8: Individual subject parameter values for tracking model with precision compensatory loop.

Subject	Run	K_f	τ_{Lf}	τ_{LLf}	τ_{If}	τ_{ILf}	Correlation
A	1	-0.038	-5.72	-5.31	4.98	2.16	0.82
	2	-0.017	-21.85	-1.55	4.42	1.06	0.91
	3	-0.010	-33.59	-2.08	3.17	2.10	0.90
B	1	-0.023	-14.84	-14.40	8.44	8.25	0.67
	2	-0.027	-8.35	-8.09	4.43	4.37	0.84
	3	0.001	399.01	-3.26	3.02	2.99	0.86
C	1	-0.039	-12.96	-1.19	8.58	0.36	0.89
	2	-0.021	-17.86	-0.92	4.56	0.40	0.90
	3	-0.020	-18.50	-0.83	4.66	0.29	0.89
D	1	-0.012	-30.61	-1.18	3.96	1.09	0.90
	2	-0.013	-30.40	-0.74	3.50	0.88	0.93
	3	-0.010	-38.87	-0.71	3.71	0.56	0.92
E	1	-0.016	-29.95	-0.61	4.61	0.24	0.88
	2	-0.015	-33.04	-0.61	5.76	0.20	0.87
	3	-0.020	-26.66	-0.72	6.85	0.20	0.89

Table 9: Individual subject parameter values for tracking model with bimodal compensatory loop.

D Joystick dynamics

Joystick dynamics were investigated with the assumption that they can be modelled as a second order system with fixed stiffness and damping originating from the mechanical springs and dampers. The transient peak ratio method was used for parameter identification. The transient response required for this process was obtained by simply deflecting the stick fully aft and releasing it. The time history immediately after the release was then used for the process. The calculations in the identification are presented in Table 10.

t	Δt	D	D_{n+1}/D_n	$ln(D_{n+1}/D_n)$	ω_d	ω_n
0.44	-	-	-	-	-	-
0.53	0.09	1.39	0.73	-0.32	69.81	70.47
0.61	0.08	1.01	0.71	-0.34	78.54	79.28
0.70	0.09	0.72	0.64	-0.44	69.81	70.47
0.78	0.08	0.46	0.63	-0.46	78.54	79.28
0.83	0.05	0.29	0.55	-0.59	125.66	126.84
0.90	0.07	0.16	-	-	89.76	90.60

Table 10: Calculation of joystick damping and natural frequency.

In this case, the damping and stiffness were found to be 0.14 and 86rad/s respectively. Therefore, the following second-order transfer function can be used to model the joystick dynamics:

$$P_j(s) = \frac{7396}{s^2 + 24s + 7396} \tag{18}$$